ZIBELINE INTERNATIONAL™ PUBLISHING

ISSN: 2616-4302 (Online)
CODEN: AMMCFL

Acta Mechanica Malaysia (AMM)

DOI: http://doi.org/10.26480/amm.01.2022.06.10

RESEARCH ARTICLE

EFFECT OF THE OUTLET ORIFICE ON THE COOLING SYSTEM OF HEAT EXCHANGER

Ismail Tlanbout, Houssem Laidoudi*

Laboratory of Sciences and Marine Engineering (LSIM), Faculty of Mechanical engineering, USTO-MB, BP 1505, El -Menaouer, Oran 31000, Algeria.
**Corresponding author E-mail: Houssem.laidoudi@univ-usto.dz*

ARTICLE DETAILS

Article History:

Received 15 Deecember 2021
Accepted 17 January 2022
Available online 25 January 2022

ABSTRACT

This work aims to give new results about the effect of the outlet opening of heat exchanger on its cooling quality. Three outlet opining locations have been studied in order to determine the best location that maximizes the efficiency of the heat transfer. The flow velocity at the inlet of the heat exchanger was also studied. It is worth noting that the research was carried out in a numerical way using ANSYS-CFX simulator. The latter solves both of energy and momentum equations using finite-volume method. Three pertinent parameters are considered here: the velocity of the flow at the inlet port of heat exchangers was controlled in terms of Reynolds number in the range 5 to 40. The pattern and the intensity of thermal transfer, the latter being controlled by the Richardson number selected between the values 0 and 1. The simulation was done for a simple and incompressible fluid. The results of this research showed that there is a possibility to raise the efficiency the heat exchanger if the outlet hole is placed at the bottom of the right side.

KEYWORDS

Mixed convection, micro-system, thermal buoyancy, circular exchanger, air flow, incompressible fluid.

1. INTRODUCTION

The study of cooling system is one of the most important modern and ancient studies because of its importance in many industrial and engineering domains, among which we mention the following: the micro-systems, cooling electronic components, heat exchangers, cooling towers, nuclear reactors and so on. Studies have shown that there are a number of factors affecting the cooling process, and these factors are grouped into the geometry of the system, the quality of the fluid used in the cooling, as well as the heat transfer pattern. In this part of the research, we present a group of the most recent studies that have completed, including the following: studied the cooling of two heated cylinders of square form in rectilinear channel (Chatterjee and Amiroudine, 2010). The studied pertinent parameters are: the flow velocity at the inlet of channel which expressed by the Reynolds number (= 1 to 30); the thermo-physical quality of the fluid which expressed by Prandtl number (= 0.7 to 100) and finally the pattern of the heat transfer which is mixed convection and the studied range of Richardson number is (= 0 to 1).

The results give a general understanding of the flow in the studied system. Numerically, analyzed the cooling process of air flow in square container involving a heated square cylinder (Moraga et al., 2010). The simulations were done in unsteady state with a laminar regime. The thermo-physical characteristics of the air were depended on the temperature. Also, the thermal transfer in this work is mixed convection. A study the cooling process of two circular cylinders in square chamber (Laidoudi and Makinde, 2021). The chamber has a single orifice for the flow inlet and other orifice for the flow outlet. The examined parameters are the *Ri* and *Re*. It was concluded that the flow becomes instable when the flow velocity and/or thermal buoyancy increase. Also, the values of these studied numbers had an influence on cooling process. There are also other research with the same principle in this field (Laidoudi, 2020a; Zeitoun et al., 2011; Chatterjee and Mondal, 2012; Rashidi et al., 2016; Outokesh et al., 2020; Yadegari and Khoshnevis, 2021; Derakhshandeh and Gharib, 2020; Sasmal and Chhabra, 2012; Soares et al., 2010; Ribeiro et al., 2014; Selimefendigil and Oztop, 2014; Sarkar et al., 2011; Krishnan and Aravamudan, 2013).

The heat transfer from a solid body to a fluid called convection, and it has three aspects: the first one is the forced convection, which is when the fluid is initially moved using a pumping device such as a pump for liquids and a fan for gases; the second type is the natural convection (Sivakumar et al., 2006; Lin, 2013; Dhimana et al., 2008; Rao et al., 2011; Laidoudi, 2020b; Almensoury et al., 2021; Laidoudi, 2020c; Hærvig and Sørensen, 2020). In this case the fluid moves by the force of gravity, that is, the hot spots of the fluid move upwards due to its lack of density; the last pattern is called the mixed convection, which combines the first type with the second in one system (Laidoudi and Ameur, 2020; Ma et al., 2020; Khan and Zaib, 2020; Laidoudi and Bouzit, 2018; Mokeddem et al., 2019). In the case of mixed convection, the ratio between natural and forced convections is expressed by the Richardson number. That is, if the value of *Ri* = 0, this means that the convection is only forced.

But if the value of *Ri* limited between 0 and 1, the effect of forced convection is more than the effect of natural convection. If the value of *Ri* is greater than 1 this indicates that the natural convection activity is more than the forced convection activity. The effect between them is equal if the value of *Ri* = 1. Based on the examination of previous works, it turns out that the study of the effect of heat transfer inside a circular chamber has not studied before, so we decide to study this topic, which has applications in many fields. The studied parameters in this investigation are: the position of the outlet port and the effect of the values of Ri and Re numbers. The purpose of this work is to find the values of the number Nusselt in terms of the studied parameters; interpretation of the effect of exit port location on thermal behavior; finding the best location of the exit hole that allows to increase the efficiency of the heat exchanger.

2. PRESENTATION OF THE STUDIED DOMAIN

Quick Response Code	Access this article online	
	Website: www.actamechanicamalaysia.com	**DOI:** 10.26480/amm.01.2022.06.10

Cite The Article: Ismail Tlanbout, Houssem Laidoudi (2022). Effect of The Outlet Orifice on The Cooling System of Heat Exchanger. *Acta Mechanica Malaysia, 5(1): 06-10.*

The studied system is described in the Figure 1. The cooling system consists of a circular container with two openings, the first (on the left at the top) for the fluid to enter and the second for its exit. The diameter of the container is (*D*). The container contains a circular cylinder of diameter (*d*) and with high temperature (T_w). The ratio between d and *D* gives the value $d/D = 0.4$. *l* expresses the width of the entry and exit orifices and is equal to the value $l = 0.1D$. The flow has a cold temperature (T_{in}) and initial velocity u_{in}. Meanwhile, the walls of the outer container are adiabatic. The selected positions of the exit orifice are indicated respectively in the fig. 1 (a), (b) and (c).

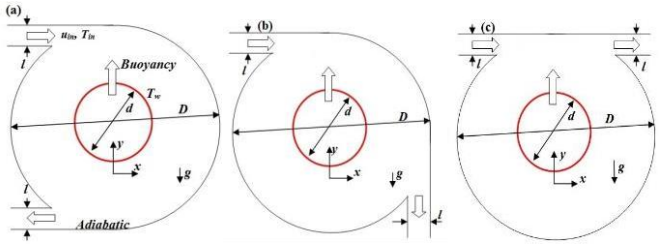

Figure 1: Studied geometry with its modifications.

3. Mathematical Formulation and Boundary Conditions

The basic equations for the present research are the continuity, momentum and energy. The energy equation is coupled with the momentum equation to describe the effect of temperature on the fluid density. The simulations are in steady state and for laminar regime. Therefore, the partial forms of these equations of present topic are written in non-dimensional form as:

$$\frac{\partial U}{\partial X}+\frac{\partial V}{\partial Y}=0 \tag{1}$$

$$U\frac{\partial U}{\partial X}+V\frac{\partial U}{\partial Y}=-\frac{\partial P}{\partial X}+\frac{1}{Re}\left(\frac{\partial^2 U}{\partial X^2}+\frac{\partial^2 U}{\partial Y^2}\right) \tag{2}$$

$$U\frac{\partial V}{\partial X}+V\frac{\partial V}{\partial Y}=-\frac{\partial P}{\partial Y}+\frac{1}{Re}\left(\frac{\partial^2 V}{\partial X^2}+\frac{\partial^2 V}{\partial Y^2}\right)+Ri\theta \tag{3}$$

$$U\frac{\partial \theta}{\partial X}+V\frac{\partial \theta}{\partial Y}=\frac{1}{PrRe}\left(\frac{\partial^2 \theta}{\partial X^2}+\frac{\partial^2 \theta}{\partial Y^2}\right) \tag{4}$$

All parameters in the governing equations are dimensionless, and they are obtained as:

$$(X,Y)=\frac{(x,y)}{d},(U,V)=\frac{(u,v)}{u_{in}},P=\frac{p}{\rho u_{in}^2},\theta=\frac{(T-T_{in})}{T_w-T_{in}} \tag{5}$$

where *X*, *Y* are components of direction in Cartesian coordinate system; *U*, *V* are velocity components; *P* and θ are the pressure and temperature respectively.

There are some dimensionless numbers that are appeared in the basic equations: Prandtl number (*Pr = 0.71*), Richardson number (*Ri*) and Reynolds number (*Re*). Their expression:

$$Re=\frac{u_{in}d}{\nu},Gr=\frac{g\beta_T\Delta T d^3}{\nu^2},Ri=\frac{Gr}{Re^2},Rr=\frac{\nu}{\alpha} \tag{6}$$

where *Gr* is Grashof number. The parameters of these numbers are: β_T is volume expansion coefficient; *g* is the gravitational acceleration; ν is the kinematic viscosity and α is thermal diffusivity.

The local value of Nusselt number on the surface is calculated as:

$$Nu_l=\frac{hd}{k}=-\frac{\partial\theta}{\partial n_s} \tag{7}$$

The equation shows the relationship between the Nusselt number, the coefficient of convection (*h*) and the gradient of temperature. *K* indicates the thermal conductivity of the fluid and n_s unit vector on the surface.

The integration of the values of the local Nusselt number gives the average value of this number as:

$$Nu=\frac{1}{S}\int_s Nu_l ds \tag{8}$$

The boundary conditions used for this investigation are:

- At the inlet orifice:

$$U=1,V=0,\theta=0 \tag{9}$$

- At the outlet orifice:

$$\frac{\partial U}{\partial X}=0,\frac{\partial V}{\partial X}=0,\frac{\partial \theta}{\partial X}=0 \tag{10}$$

- On cylinder surface:

$$U=0,V=0,\theta=1 \tag{11}$$

- On container surfaces:

$$U=0,V=0,\frac{\partial\theta}{\partial n}=0 \tag{12}$$

No-slip condition is adopted on the walls of the geometry to perform the effect of dynamic viscosity.

4. Numerical Methodology and Validation Test

In numerical work, the work is divided into two main parts, the stage of creating the mesh for the studied geometry, and the second, the simulation process. Gambit was used for the first stage. Triangular elements with irregular distribution were chosen to create the grid. The mesh elements are largely concentrated around the inner cylinder because of the fluid layers are very sensitive Figure 2. The mesh elements have been selected based on the relevant study (grid independency test). The results of the test are clearly represented in Table 1. The grid M2 of 211000 elements is satisfactory for this investigation. The second part of this work is accomplished by ANSYS-CFX code. This package uses the volume finite method to solve the basis equations (1-4).

High resolution discretization scheme is used for the resolution of the convective terms and SIMPLEC algorithm is used velocity-pressure coupling. 10^{-8} and 10^{-6} values are chosen for the relative error of the momentum and energy equation, respectively. This section includes also the validation test. This step is necessary to proof the ability of present methodology for obtaining accurate results. Therefore, we did the same work that was achieved by (Chatterjee and Amiroudine, 2010). The work is about a flow in straight channel with two heated square cylinders in tandem configuration. The conditions of the simulations are *Ri* = 0.25, *Re* = 1 to 30 and *Pr* = 10. The results are compared to the Nusselt number for the first and second cylinders. The results of the comparison are in Table 2. A good agreement is determined between the results. We conclude from this that our method used in this work has the ability to find accurate values.

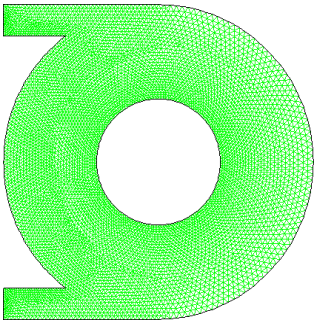

Figure 2: Grid structure for the present work.

Table 1: The grid independency test for Ri = 0, Re = 10 and Pr = 0.71.

Mesh	**M1**	**M2**	**M3**
Elements	105000	211000	422000
Nu	0.52453	0.51234	0.51321
Error %	2.32	0.17	-

Table 2: Validation test

Re	First cylinder (upstream)			Second cylinder (downstream)		
	Nu	*Nu* Chatterjee and Amiroudine, 2010	difference %	*Nu*	*Nu* Chatterjee and Amiroudine, 2010	difference %
1	1.79	1.8	0.56	1.26	1.3	3
10	3.94	3.94	0	2.59	2.6	0.4
30	6.37	6.4	0.47	3.78	3.83	1.3

5. Results and Discussion

The results of this work are divided into three parts according to the location of the exit orifice. Since each time, we display the streamlines, followed by the isotherms, and then the values of average *Nu* in terms of the values of the studied parameters. Figure 3 presents the streamlines inside the studied domain for the first case, where the exit hole is in the lower left side. The streamlines changes are presented in terms of values of Richardson and Reynolds number. The working fluid is air, so the Prandtl number value is 0.71. The red color represented on the streamlines indicates the maximum value of the velocity, while the blue color indicates the minimum value. It is clearly noticed that as the value of Richardson number increases, the shape of flow becomes less stable with the presence of many vortices indicating the presences of fluid stagnation area. The important not here is that since the value of Richardson number (Ri = 0), the fluid turns around the inner cylinder from the right side due to the centrifuge force, but with the increase from the value of Richardson the flow changes its direction to pass around the inner cylinder from the left side. The change is what led to the emergence of vertices on the right side. This change in the direction of the fluid is due to the effect of thermal buoyancy force that caused the hot fluid layers to move upwards, which causes the fluid's path to be closed on the right side, and this causes the flow to move towards the left side.

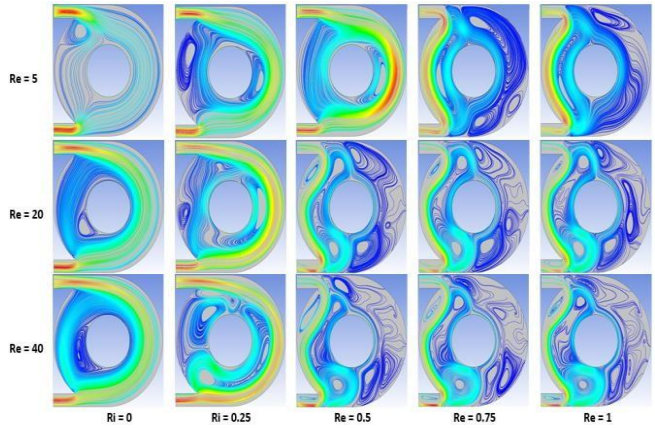

Figure 3: Streamlines in the first configuration for different Ri and Re.

Figure 4 shows the isotherms inside the first geometrical configuration with different values of Ri et Re. the thermal distribution shows the same behavior that was observed from the previous streamlines. In addition to this, it is also noted that the gradient temperature around the heated cylinder increases with the increase of the Richardson number and the Reynolds number, which indicates that the heat transfer increases with the increase of these two numbers.

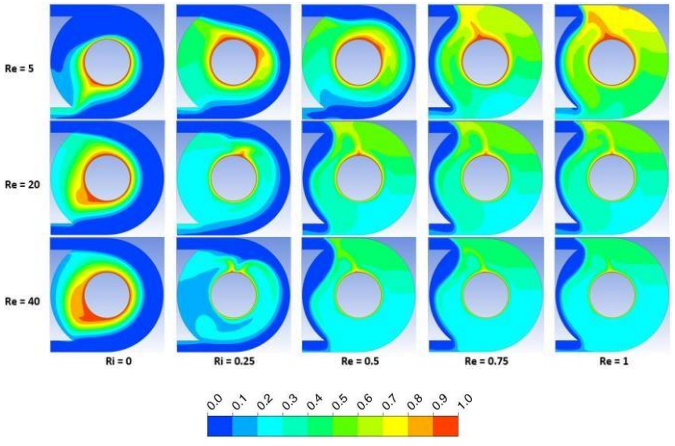

Figure 4: Isotherms in the first configuration for different Ri and Re.

Figure 5 shows the values of Nusselt number of the heated obstacle versus Ri and Re for the first position of exit orifice. It is clear that Nu increases with increasing *Re* and *Ri*. Due to the fact that the increase of Re and/or Ri increases the velocity of the flow in the studied domain which increases the evacuation of thermal energy from the obstacle surface to the fluid flow. Therefore, heat transfer becomes important. Furthermore, for the case of forced convection (*Ri* = 0) increase of Re decreases the value of *Nu* number. On other hand, for the case of mixed convection, increase the value of *Re* increases the average *Nu*. Thermal transfer decreases in the first case because of the centrifugal force that pushes the fluid towards the outer wall, which reduces the fluid's velocity near the inner obstacle wall.

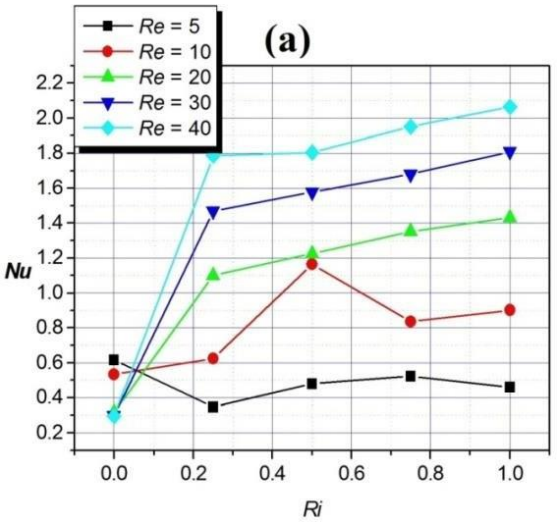

Figure 5: Variation of Nusselt number with Ri and Re for the first geometrical configuration.

Figures 6, 7 and 8 are for the second geometrical configuration where the exit orifice is on the lower right side. Figure 6 shows the contours of the streamlines in terms of *Ri* and *Re* numbers. The flow is more stable in the case of forced convection with the appearance of a vortex on the left side. This vortex moves downwards as the Reynolds number increases. Just like the first case, the flow changes direction from the upper side to the lower side by the effect of thermal side.

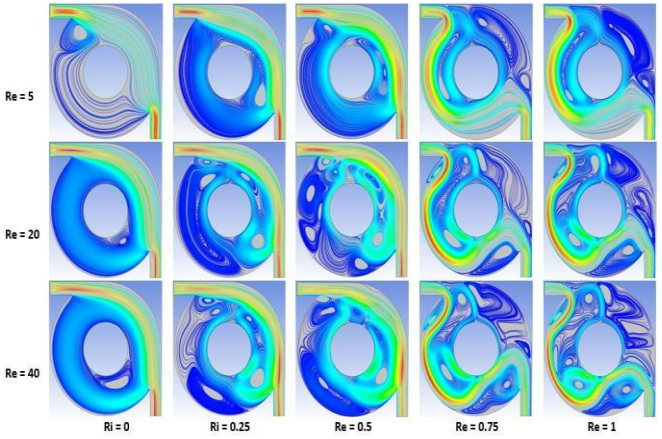

Figure 6: Streamlines in the second configuration for different Ri and Re

Figure 7 shows the isotherms in the second configuration. These isotherms reflect exactly the same behavior that was inferred from the examination of streamlines. For the case of *Ri* = 0. The temperature gradient decrease with increasing *Re*. On other hand, it increases for the case of mixed convection.

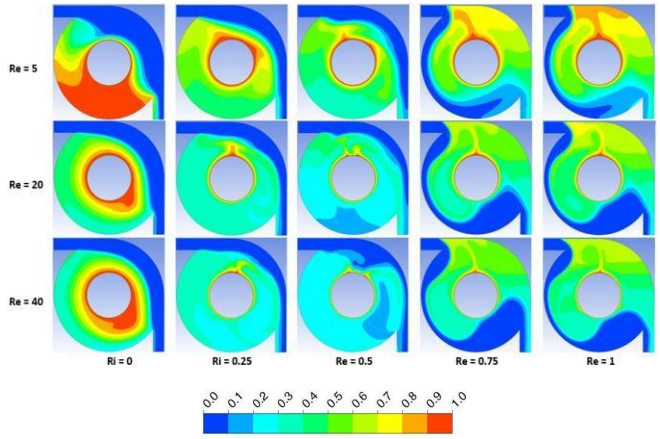

Figure 7: Isotherms in the second configuration for different Ri and Re.

Figure 8 show plotted graphs of the variation on Nusselt number as function of Ri and Re. like the first case, the value of Nusselt number decreases with increasing Re in the case of Ri = 0. But it increases again when Ri ≠ 0. In general, the Nusselt values for the inner cylinder for this case are slightly better than those for the first case.

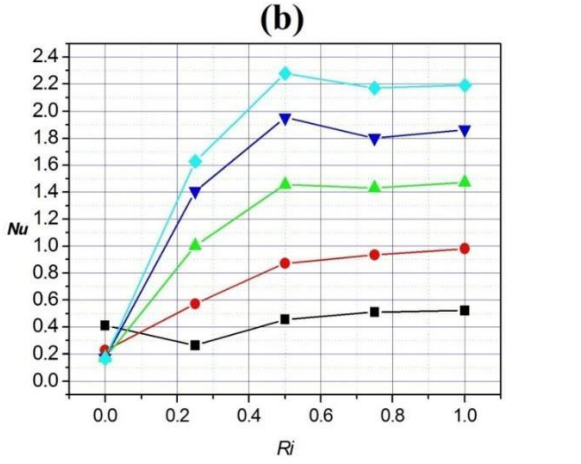

Figure 8: Variation of Nusselt number with Ri and Re for the second geometrical configuration.

Figures 9, 10 and 11 represent the results of the third configuration where the outlet orifice is located to the right at the top. The streamlines in Figure 9 shows that the presence of the vortex on the left side, then it moves to right side when the *Re* value is increased. It is also shown that the effect of thermal buoyancy. It is also noticed that the effect of thermal buoyancy helped the flow to move downwards, which helps in raising the heat transfer. As in the previous cases, thermal buoyancy reduces the stability of the flow within the system. Figure 10 shows the isotherms in third configuration with *Ri* and *Re*. In general, it is noticed that the increase in the fluid velocity value at the inlet port or increase in thermal buoyancy effect makes the thermal layers around the cylinder more concentrated, which indicates the high value of temperature gradient around the obstacle.

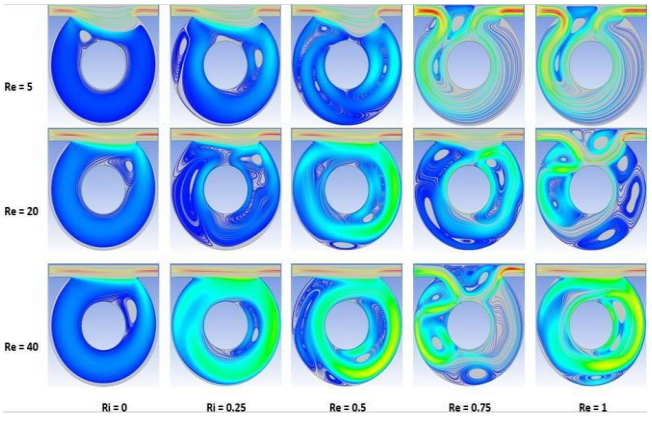

Figure 9: Streamlines in the third configuration for different Ri and Re

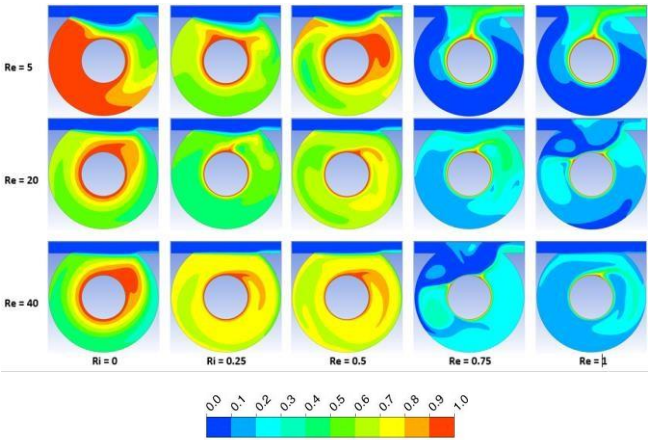

Figure 10: Isotherms in the third configuration for different Ri and Re

Figure 11 shows the variation of *Nu* number of the third configuration as function of Ri and Re. it is clear that, for the case of mixed convection, there is a significant effect of Re number on the Nu. In this case, it is noticed that the effect of Reynolds and Richardson numbers on Nusselt value is sometimes high and sometimes decreasing. Accordingly, we conclude this third case important in cases of thermal insulation.

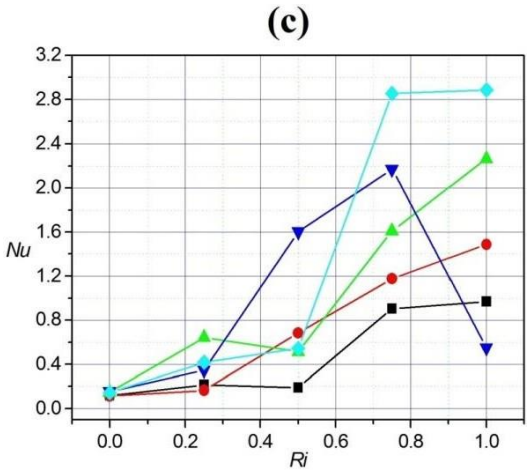

Figure 11: Variation of Nusselt number with Ri and Re for the third geometrical configuration.

6. Conclusion

In this work, we dealt with a numerical simulation of a flow inside heat exchangers. This exchanger is used in many industrial applications, especially cooling of micro-systems. The parameters studied here concern the design of the system and the mode of operation. The changes in the geometry study the position of the exit orifice and its effect on the quality of cooling, while the operating conditions study the effect of flow velocity and the heat transfer pattern on the quality of cooling. This investigation enabled us to conclude the following points:

- The position of the exit orifice significantly effects quality of cooling. The results showed that the second position of the orifice is better than the first and the last in terms of heat transfer efficiency.
- For the first and second configurations and for *Ri* = 0, increase in the value of *Re* decreases the value of Nu. On other hand, when *Ri* ≠ 0, increase in Re promotes the rate of heat transfer.
- The last position has the difficulty of the cooling process and is the worst configuration.
- The buoyancy is the major factor that determines the structure of the flow in the domain.

References

Almensoury, M.F., Hashim, A.S., Hamzah, H.K., Ali, F.H., 2021. Numerical investigation of natural convection of a non-Newtonian nanofluid in an F-shaped porous cavity. Heat Transfer, 50, Pp. 2403–2426.

Chatterjee, D., Amiroudine, S., 2010. Two-dimensional mixed convection heat transfer from confined tandem square cylinders in crossflow at low Reynolds numbers. Communications in Heat and Mass Transfer, 37, Pp. 7–16.

Chatterjee, D., Mondal, B., 2012. Forced convection heat transfer from an equilateral triangular cylinder at low Reynolds numbers. Heat Mass Transfer, 48, Pp. 1575–1587.

Derakhshandeh, J.F., Gharib, N. 2020. Laminar flow instabilities of a grooved circular cylinder. Journal of the Brazilian Society of Mechanical Sciences and Engineering, 42, Pp. 580.

Dhimana, A.K., Chhabra, R.P., Eswaran, V., 2008. Steady flow across a confined square cylinder: Effects of power-law index and blockage ratio. J. Non-Newtonian Fluid Mechanics, 148, Pp. 141–150.

Hærvig, J., Sørensen, H., 2020. Natural convective flow and heat transfer on unconfined isothermal zigzag-shaped ribbed vertical surfaces. Communications in Heat and Mass Transfer, 119, Pp. 104982.

Khan, U., Zaib, A., Mebarek-Oudina, F. 2020. Mixed convective magneto flow of SiO2–MoS2/C2H6O2 hybrid nanoliquids through a vertical stretching/shrinking wedge: stability analysis. Arabian Journal for Science and Engineering, 45, Pp. 8817–8876.

Krishnan, S., Aravamudan, K., 2013. Simulation of non-Newtonian fluid-food particle heat transfer in the holding tube used in aseptic processing operations. Food and Bioproducts Processing, 91, Pp. 129–148.

Laidoudi, H., 2020a. Upward flow and heat transfer around two heated circular cylinders in square duct under aiding thermal buoyancy. Journal of the Serbian Society for Computational Mechanics, 14, Pp. 116–131.

Laidoudi, H., 2020b. Buoyancy-driven flow in annular space from two circular cylinders in tandem arrangement Metallurgical and Materials Engineering, 26, Pp. 87–102.

Laidoudi, H., 2020c. Natural convection from four circular cylinders in across arrangement within horizontal annular space. Acta Mechanica et Automatica, 14, Pp. 98–102.

Laidoudi, H., Ameur, H., 2020. Investigation of the mixed convection of power-law fluids between two horizontal concentric cylinders: Effect of various operating conditions Thermal Science and Engineering Progress, 20, Pp. 100731.

Laidoudi, H., Bouzit, M., 2018. The effects of aiding and opposing thermal buoyancy on downward flow around a confined circular cylinder. Periodica Polytechnica Mechanical Engineering, 62, Pp. 42–50.

Laidoudi, H., Makinde, O.D., 2021. Computational study of thermal buoyancy from two confined cylinders within a square enclosure wifth single inlet and outlet ports. Heat Transfer, 50, Pp. 1335–1350.

Lin, C.N., 2013. Enhanced heat transfer performance of cylindrical surface by piezoelectric fan under forced convection conditions. International Journal of Heat and Mass Transfer, 60, Pp. 296–308.

Ma, Y., Mohebbi, R., Rashidi, M.M., Yang Z., 2019. Koo–Kleinstreuer–Li correlation for simulation of nanofluid natural convection in hollow cavity in existence of magnetic field. Journal of Thermal Analysis and Calorimetry, 137, Pp. 1413–1429.

Mokeddem, M., Laidoudi, H., Makinde, O.D., Bouzit, M., 2019. 3D Simulation of incompressible poiseuille flow through 180° curved duct of square cross-section under effect of thermal buoyancy. Periodica Polytechnica Mechanical Engineering, 63, Pp. 257–269.

Moraga, N.O., Andrade, M.A., Vasco, D.A., 2010. Unsteady conjugate mixed convection phase change of a power law non-Newtonian fluid in a square cavity. International Journal of Heat and Mass Transfer, 53, Pp. 3308–3318.

Outokesh, M., Ajarostaghi, S.S.M., Bozorgzadeh, A., Sedighi, K., 2020. Numerical evaluation of the effect of utilizing twisted tape with curved profile as a turbulator on heat transfer enhancement in a pipe. Journal of Thermal Analysis and Calorimetry, 140, Pp. 1537–1553.

Rao, P.K., Sahu, A.K., Chhabra, R.P., 2011. Momentum and heat transfer from a square cylinder in power-law fluids. International Journal of Heat and Mass Transfer, 54, Pp. 390–403.

Rashidi, S., Bovand, M., Esfahani, J.A., 2016. Opposition of Magnetohydrodynamic and AL2O3–water nanofluid flow around a vertex facing triangular obstacle. Journal of Molecular Liquids, 215, Pp. 276–284.

Ribeiro, V.M., Coelho, P.M., Pinho, F.T., Alves, M.A., 2014. Viscoelastic fluid flow past a confined cylinder: Three-dimensional effects and stability. Chemical Engineering Science, 111, Pp. 364–380.

Sarkar, S., Dalal, A., Biswas, G., 2011. Unsteady wake dynamics and heat transfer in forced and mixed convection past a circular cylinder in cross flow for high Prandtl numbers. International Journal of Heat and Mass Transfer, 54, Pp. 3536–3551.

Sasmal, C., Chhabra, R.P., 2012. Effect of aspect ratio on natural convection in power-law liquids from a heated horizontal elliptic cylinder. International Journal of Heat and Mass Transfer, 55, Pp. 4886–4899.

Selimefendigil, F., Oztop, H.F., 2014. Forced convection of ferrofluids in a vented cavity with a rotating cylinder. International Journal of Thermal Sciences, 86, Pp. 258–275.

Sivakumar, P., Bharti, R.P., Chhabra, R.P., 2006. Effect of power-law index on critical parameters for power-law flow across an unconfined circular cylinder. Chemical Engineering Science, 61, Pp. 6035–6046.

Soares, A.A., Ferreira, J.M., Caramelo, L., Anacleto, J., Chhabra, R.P., 2010. Effect of temperature-dependent viscosity on forced convection heat transfer from a cylinder in crossflow of power-law fluids. International Journal of Heat and Mass Transfer, 53, Pp. 4728–4740.

Yadegari, M., Khoshnevis, A.B., 2021. Numerical and experimental study of characteristics of the wake produced behind an elliptic cylinder with trip wires. Iranian Journal of Science and Technology, Transactions of Mechanical Engineering, 45, Pp. 265–285.

Zeitoun, O., Ali, M., Nuhait, A., 2011. Convective heat transfer around a triangular cylinder in an air cross flow. International Journal of Thermal Sciences, 50, Pp. 1685–1697.